01,05

Similarity of THz radiation excitation mechanisms in magnetic nanocontacts and in nanoheterostructure with heavy metal Mo

© E.A. Vilkov, S.G. Chigarev, O.A. Byshevsky-Konopko

Kotelnikov Institute of Radio Engineering and Electronics, Russian Academy of Sciences, Fryazino Branch, Fryazino, Moscow Region Russia

E-mail: chig50@mail.ru

Received April 12, 2023
Revised June 22, 2023
Accepted July 13, 2023

The modes of occurrence of Three-band electromagnetic oscillations during the flow of current in magnetic nanocontacts and in a heterogeneous Fe/Mo structure with a heavy metal nanofilm are compared, and the similarity of the dependences of the change in radiated power on the change in current in the region of radiation occurrence is established. Based on this, a conclusion is made about the identity of the processes of THz radiation formation in the structures under study and the possibility of spreading physical ideas about the excitation of THz radiation during spin injection by current in the case of a heterogeneous Fe/Mo structure with a heavy metal nanofilm.

Keywords: THz radiation, spin-polarized current, anisotropic exchange interaction, Dzyaloshinsky–Moriya interaction.

DOI: 10.61011/PSS.2023.09.57103.60

1. Introduction

The study of THz radiation covering the frequencies from fractions to tens terahertz has been of high interest lately [1–3]. However, its wide use in research and technology is hindered by a lack of available, reliable and space-saving THz radiation sources and detectors operated in a wide temperature range. Therefore, it is important to search for new concepts of radiation generation and detection in this frequency range. For this, the use of spintronics concepts is highly promising.

Thus, [4,5] studied a lamellar thin-film structure Pt — antiferromagnetic (AFM) material with electrical conductivity current in the platinum layer. In such structure, antiferromagnetic sublattice bevel and rotation is observed under spin current induced in the platinum layer due to spin-orbital scattering of conductivity electrons. And generation of 0.5 to 2 THz radiation is observed due to nonuniform rotation of the AFM sublattices caused by crystalline anisotropy of AFM.

Generation of terahertz radiation due to the conductivity electron transition between spin subbands in noncollinear ferromagnet with helicoidal magnetic structure was discussed in [6]. In this case, spin-nonequilibrium electrons shall be pumped into the radiation from a ferromagnetic injector. Coupling of spin and orbital degrees of freedom in the offered system is achieved due to spatially nonuniform noncollinear magnetization distribution. Due to this, sd-exchange interaction constant will depend on the quasi-momentum of d- or f-electrons.

Other approach associated with the use of structures formed by thin-film contacts was discussed, for example, in [7–9]. Formation of electromagnetic radiation in such structures is observed during spin injection by current with density more than 10^6 A/cm^2 (see, for example, [10–16]). In this case, focus was made on sd-exchange interaction of conductivity electrons with the lattice magnetic field resulting in splitting of spin-energy subbands by energy and formation of Fermi quasi levels in them. As a result, conditions occur for electromagnetic radiation excitation due to interband radiative spin-flip transitions [13–15] when conductivity electrons are exposed to the external signal.

Radiation observed by us on ~ 7 THz frequencies in a heterostructure with Mo heavy metal film contacting with Fe layer when current with density more than 10^6 A/cm^2 flows through the heterostructure [17] is believed to serve as extension of the concepts of spin-injection mechanism of THz radiation. By our tentative assumption, this radiation was associated with occurrence of weak magnetism in a heavy metal layer and with the Dzyaloshinski–Moriya interaction [18,19] resulting in spin-flip transitions of conductivity electrons between spin-split energy subbands similar to that observed in magnetic nanojunctions [7,16]. However, application of concepts developed and used to describe the process in magnetic nanojunctions during spin current injection such as „spin-energy subband splitting“, „Fermi quasi levels“, „radiative spin-flip transitions“ to formation of THz radiation in a Mo heterostructure requires more detailed confirmation.

Solution of this issue is provided herein by comparison of experimentally measured dependences of radiation power on current during generation of THz radiation in Mo/Fe and Fe/Fe junctions, and by comparison of physical representations of radiation generation in these junctions as described in [16] and [17].

2. Experiment

THz radiation excitation modes in Fe/Mo and Fe/ferromagnetic junctions were studied using the radiation source with „rod-film“ [20] structure whose scheme is shown in Figure 1. The radiation source used the samples prepared for experiments at IPTM RAS (Tchernogolovka), which consisted of 20 nm Mo films, 30 nm and 60 nm Fe films and 30 nm Fe_3O_4 films grown on a sapphire *R*-plane by the ultrahigh vacuum pulsed laser vaporization method.

To represent greater generality of the observed effects, Fe films with various thicknesses were used. Since the film thickness defines the degree of loss of THz radiation, then, when a thicker film is used, the recorded power is lower and the signal itself is less stable, which nevertheless does not disturb the general pattern of radiation generation, as shown below.

A DC source with smooth adjustment of stabilized voltage applied to the test radiation source was used as power supply. The radiation generated in the rod-film contact point was focused by the high-resistivity silicon meniscus lens. The signal was recorded by „Tydex“ Golay cell. Analog values for further treatment were digitized using AKTAKOM ASK-3117 storage oscilloscope. Measurements were carried out in the starting current region with gradual continuous increase of voltage applied to the radiation source and, therefore, with continuous current increase. Noise level in the measurements did not exceed 5% of the measured value. Roughness on the resulting curves was „smoothed“ by spline interpolation.

Figure 2 shows the power measurements with smooth continuous increase of current penetrating the Mo/Fe and Fe/Fe heterostructures.

The Mo film thickness was 20 nm, the Fe film thickness was 60 nm. As shown in the Figure, generation of radiation using the Mo/Fe junction (curve *1* in Figure 2) is abrupt, i.e. when the current is increased, generated radiation causes power variation from 0 to 2 μW in a narrow current

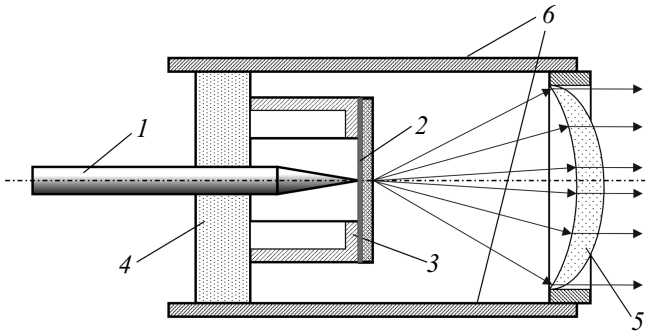

Figure 1. Spin injecting radiation source with „rod−film“ structure. *1* — ferromagnetic rod (Fe) with tip diameter 10−50 μm, *2* — Mo or ferromagnetic film on dielectric substrate, *3* — substrate holder, *4* — dielectric pad of the injector, *5* — focusing meniscus lens, *6* — lens holder. Arrows show the radiation flux.

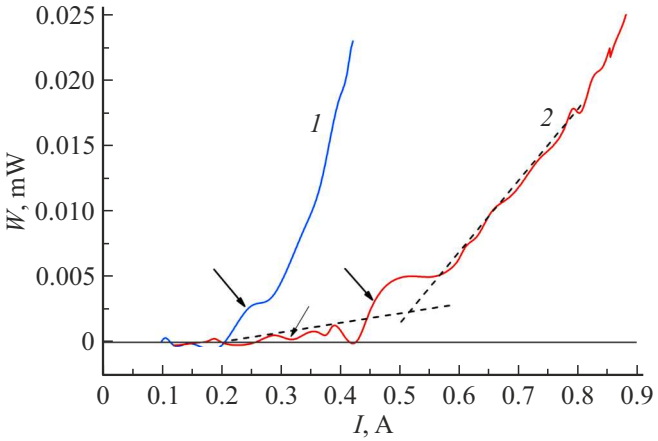

Figure 2. Dependence of the radiation power *W* on the spin injecting radiation source current *I* with „rod−film“ structure when the Mo heavy metal (curve *1*) and Fe film (curve *2*) is used in it.

range 0.23−0.235 A (abrupt power change is shown by the arrow) with subsequent gradual power increase with further current increase. On the other hand, when a signal appears in the Fe/Fe junction, the signal exceeds the zero level at 0.19 A with subsequent smooth signal increase up to 2.1 μW at 0.38 A. In this case, on the initial section of the curve $W(I)$, power increase from 0 to 2.1 μW takes place when the current increases by a factor of 2 from 0.19 to 0.38 A. The power further changes from 2.1 to 5 μW, by a factor of more than 2 when the current changes by only 0.02 A ($\sim$ 5%). Such relatively abrupt change of the power in 0.39 A region (shown by a bold arrow in the figure) is similar to abrupt power change observed when using the Mo film. After abrupt power change, smooth power increase is observed with current growth, however, the power increase slope increases compared with the previous increase slope. Power increase slope approximation is shown by dashed lines. Thus, when the Fe/Fe junction is used, abrupt power change is characterized not only by considerable power increase (by a factor of 2) with relatively small current change ($\sim$ 5%), but also by the following change in the power increase slope. This distinguishes the noted abrupt power change from the roughness of the curve of interest. As an example, roughness on curve *2* Figure 2 is shown by a thin arrow at 0.25 A. Power „dips“ observed before the abrupt power change physically justified by the occurrence of angled interband quantum transitions in the running generator requiring absorption of the third phonon particle resulting in the decrease of the radiation source temperature and, therefore, of the recorded total power. With further smooth current increase, the influence of radiation source „cooling“ [21,22] is compensated by the increase in radiation source performance characterized by the curve slope $W(I)$.

Comparison of two curves plotted for two different nanojunctions suggests that in both cases abrupt power

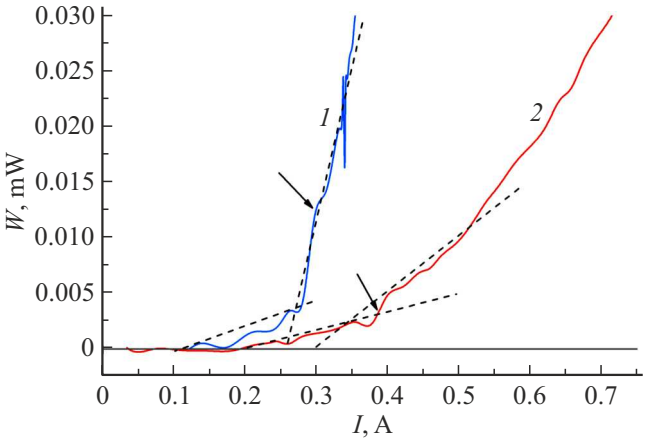

Figure 3. Dependence of the power change during current change for two magnetic junctions: curve *1* — Fe_3O_4/Fe, curve *2* — Fe/Fe. Dashed lines — linear approximation of some curve sections.

changes have qualitatively identical nature, which can be indicative of partial identity of the radiation generation processes in them.

As for explanation of various threshold currents for generation in Fe/Mo and Fe/Fe, it can be assumed roughly, by extending to the Mo film the connection between the THz signal generation performance and current density shown for the magnetic nanojunctions, that the required current density in the thinner Mo (20 nm) film is achieved at lower currents. However, a more correct answer to the question regarding the current density required for radiation excitation in the Mo film is still open until the quantitative evaluation of the radiation excitation conditions in heavy metal films is completed.

According to the study of the operating conditions of spin injection generators with magnetic junctions, the abrupt generation power increase for them in already running radiation sources is general in nature. Thus, it has been previously noted for the THz radiation in the structure using the multilayer nanowire array formed by Fe/Ni layers[21,22].

Also as an example, Figure 3 shows the electromagnetic oscillation excitation curves in the „rod−film" structures using two different ferromagnetic films: 30 nm Fe film, for which equilibrium spin polarization $P = (n_+ - n_-)/(n_+ - n_-) \sim 0.4$, where n_+ is the partial electron concentration with various spin orientation relative to magnetization of the film and 30 nm Fe_3O_4 film for which $P \sim 1$. The rod in both structures is made from Fe with tip diameter $d \sim 30\,\mu$m. This Figure shows that a qualitatively identical picture is observed for both ferromagnetic materials. First, when some current value is exceeded, for Fe $I = 0.19$ A, and for Fe_3O_4 $I = 0.1$ A, when the radiated power starts exceeding the zero level, smooth radiation power increase is observed. Second, at currents for Fe $I = 0.38$ A, and for Fe_3O_4 $I = 0.27$ A, abrupt power change is observed after which change in the curve increase slope $W(I)$ is observed in both cases. Which is demonstrated by the linear approximation of the curve $W(I)$ sections by dashed lines. It should be noted that both processes in the studied structures are observed at different currents. The observed abrupt power changes followed by increase slope change with current growth when ferromagnetic films are used may suggest that radiation occurs with another nature than the radiation that causes smooth power increase from zero in the initial generation area. It can be seen that for Fe_3O_4, a material with higher equilibrium spin polarization P, the dependence is sharper. The existing spin injection generation theory does not yet allow to perform the qualitative evaluation of the divergence of the results shown in Figure 3 for magnetic films with different equilibrium spin polarization P. Detailed consideration of the complex nature of electromagnetic oscillation excitation in the magnetic junctions is not included herein.

To identify the processes in magnetic nanocontacts and Mo/Fe heterostructure, the presence of abrupt power change in all cases is mainly focused and explained below.

3. Interpretation of findings

According to [17], excitation of THz radiation in the Mo/Fe heterostructure is explained by the occurrence of anisotropy at the layers interface and the presence of strong spin-orbit interaction in Mo resulting in occurrence of the Dzyaloshinski–Moriya (DM) type interaction for conductivity electrons at the interface with iron. anisotropy of exchange interaction between conductivity electrons and bound electrons is shown in [17] as

$$H_{\mathrm{DM}} = D_{\mathrm{SD}}(\mathbf{S}_1 \times \mathbf{S}_2), \tag{1}$$

where $\mathbf{S}_1, \mathbf{S}_2$ are conductivity electron and bound electron spin operators. Addition of a DM term (D_{SD}) to the Heisenberg Hamiltonian allowed to represent effective exchange interaction in the tensor form

$$\ddot{J} = \begin{pmatrix} J & D_{\mathrm{SD3}} & -D_{\mathrm{SD2}} \\ -D_{\mathrm{DS3}} & J & D_{\mathrm{SD1}} \\ D_{\mathrm{SD2}} & -D_{\mathrm{SD1}} & J \end{pmatrix}, \tag{2}$$

where J is the Heisenberg exchange interaction constant, D_{SD1}, D_{SD2}, D_{SD3} are the Dzyaloshinski vector components for conductivity electron and bound electron interaction. However, representations described in [17] cannot explain the threshold nature of the THz radiation excitation. Therefore, a more well-developed theory of spin ejection generation in magnetic nanojunctions will be used.

According to general representations of performance of spin injection radiation sources [7,16] formed by at least two magnetic nanolayers having significantly different magnetic characteristics (for example, magnetization orientation), the current penetrating the junction is spin-polarized in one of the layers, which is referred to as the injector. The spin-polarized current injected into the second effective

layer disturbs the equilibrium spin state in it. The spin-energy subbands in the effective layer, which have been previously balanced by spins, are expanded by energy with formation in each of the subbands of Fermi quasi levels e_{F+} and e_{F-} spaced up and down by energy relative to the Fermi equilibrium level e_F. In one of the subbands with e_{F+} „minority" spin-nonbalanced energy-excited („hot") electrons occur, and in the second subband with e_{F-} „majority" vacant energy level occur. According to [16], the Hamiltonian describing this process is written as

$$\hat{H} = \hat{\sigma}_o \cdot \frac{p^2}{2m} - \hat{\boldsymbol{\sigma}}\mathbf{I}(\hat{\mathbf{p}}) + \hat{\boldsymbol{\sigma}} \cdot \frac{e}{2c} \cdot \left(\frac{\partial \mathbf{I}}{\partial \hat{\mathbf{p}}} \mathbf{A} + \mathbf{A} \frac{\partial \mathbf{I}}{\partial \hat{\mathbf{p}}} \right). \quad (3)$$

Here, $\hat{\sigma}_o \cdot$ is the single matrix with 2×2 dimensions, $p^2/2m^*$ is the electron kinetic energy, p is the conductivity electron pulse, m^* is the effective conductivity electron mass, $\hat{\boldsymbol{\sigma}}$ is the Pauli matrix, $\mathbf{I} = \mu_B G(\mathbf{p})\mathbf{M}_2(\mathbf{r})$ is the exchange interaction energy sd, $G(\mathbf{p})$ is the exchange tensor sd with the shape similar to that described by equation (2), μ_B is the Bohr magneton, $\mathbf{A}$ is the vector potential of he external electromagnetic field.

The first two terms in equation (3) describe the radiation occurrence in magnetic junctions on the initial section with formation of Fermi quasi levels (see Figure 3), the third term describes the radiation generation process due to spin-flip transitions with abrupt power change. The third term is equal to zero only in case of medium anisotropy and is described by the matrix with non-zero off-diagonal terms

$$\hat{H}_e = -\begin{pmatrix} -J_z & -J_x - iJ_y \\ -J_x + iJ_y & J_z \end{pmatrix}. \quad (4)$$

Here

$$\mathbf{J} = \frac{e}{2c} \cdot \left(\frac{\partial \mathbf{I}}{\partial \hat{\mathbf{p}}} \mathbf{A} + \mathbf{A} \frac{\partial \mathbf{I}}{\partial \hat{\mathbf{p}}} \right)$$

is the vector whose projections form matrix (4).

Thus, like with the Mo film, the medium anisotropy in the magnetic nanojunctions predetermines transition of „hot" electrons existing in the „minority" subband to another energy subband, „majority", with spin flip by making a radiative spin-flip transition. However, for this radiative process, according to [7,8,11], it is necessary to create conditions for inverse population of spin subbands, when the concentration of „hot" electrons in the „minority" subband would exceed the electron concentration in the „majority" subband, i. e. spin polarization would have a negative value.

According to [7,8], the inverse population of spin subbands is determined by the density of current penetrating the magnetic junction. This is illustrated in Figure 4 taken from [8]. As shown in the figure, the inverse population corresponding to the negative spin polarization values $P(R)$ of the injected electron flux occurs only when particular current densities are achieved and depends on the rod polarization vs. equilibrium film polarization. Therefore, in this case, the radiative interband spin-flip transitions occur only when some current value is exceeded, i. e. the process is of a threshold current nature.

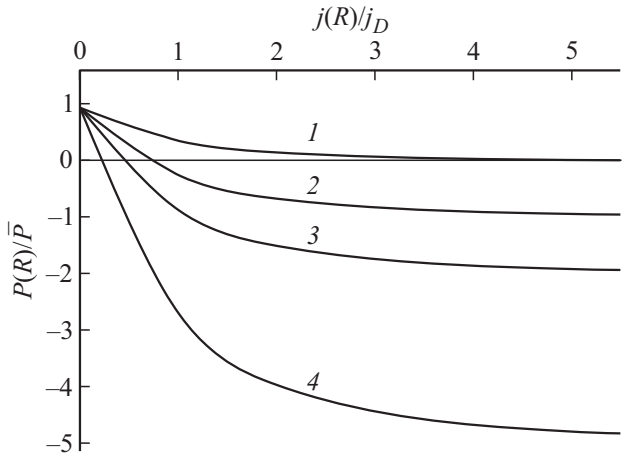

Figure 4. The spin polarization at the interface between the rod and film (assigned to the equilibrium value) $P(R)/P$ depending on (dimensionless) the current density $j(R)/j_D$ at $R/l = 20$ and different relations of rod polarization vs. equilibrium film polarization: 0 (*1*), 1 (*2*), 2 (*3*), 5 (*4*). R is the rod radius, l is the spin relaxation length.

The governing role of the medium anisotropy in the occurrence of an abrupt power change in both cases and similar formal description of the radiation processes by matrices with non-zero off-diagonal terms suggests that generation of radiation is similar in magnetic nanostructures and heterostructures with heavy metal films.

The observed in both cases power „dip" before abrupt power change, which is explained above by some decrease of the radiation source temperature associated with phonon absorption during indirect quantum transitions, may serve as an additional confirmation of radiation generation identity in these structures.

4. Conclusions

The study has experimentally determined the nature of THz radiation excitation with abrupt power change both in the nanoheterostructure with Mo heavy metal film and in magnetic junction during spin current injection due to radiative interband spin-flip transitions with varying spin orientation. In both cases, the spin-flip transitions are associated with the medium anisotropy, though they have different enabling conditions. For the Mo film, this is a strong spin-orbit interaction inducing the Dzyaloshinski–Moriya interaction at the layers interface, and for magnetic junction, this is sd-exchange interaction between the conductivity electrons and bound lattice electrons. Nevertheless, the presence of radiation with abrupt power change in both cases allows to extend the concepts of radiative spin-flip transitions developed for the spin-ejection THz radiation to the THz radiation generation process in the heterostructures with heavy metal films.

It should be noted that generation of the THz radiation during spin current injection in magnetic nanocontacts is generally more complicated in nature, and is not described herein and required additional investigations.

Acknowledgments

The authors would like to thank I.Yu. Malikov (IPTM RAS, Tchernogolovka), for the kindly provided samples for experiments, as well as L.A. Fomin (IPTM RAS, Tchernogolovka) for participation in the discussion of findings.

Funding

This study was carried out under the state assignment of the Kotel'nikov Institute of Radio Engineering and Electronics of the Russian Academy of Sciences for 2023 No. 075-01110-23-01.

Conflict of interest

The authors declare that they have no conflict of interest.

References

[1] V. Baltz, A. Manchon, M. Tsoi, T. Moriyama, T. Ono, Y. Tserkovnyak. Rev. Mod. Phys. **90**, *1*, 015005 (2018).
[2] S.S. Dhillon, M.S. Vitiello, E.H. Linfield, A.G. Davies, M.C. Hoffmann, J. Booske, C. Paoloni, M. Gensch, P. Weightman, G.P. Williams, E. Castro-Camus, D.R.S. Cumming, F. Simoens, I. Escorcia-Carranza, J. Grant, S. Lucyszyn, M. Kuwata-Gonokami, K. Konishi, M. Koch, C.A. Schmuttenmaer, T.L. Cocker, R. Huber, A.G. Markelz, Z.D. Taylor, V.P. Wallace, J.A. Zeitler, J. Sibik, T.M. Korter, B. Ellison, S. Rea, P. Goldsmith, K.B. Cooper, R. Appleby, D. Pardo, P.G. Huggard, V. Krozer, H. Shams, M. Fice, C. Renaud28, A. Seeds, A. Stöhr, M. Naftaly, N. Ridler, R. Clarke, J.E. Cunningham, M.B. Johnston. J. Phys. D **50**, *4*, 043001 (2017).
[3] F. Hellman, A. Hoffmann, Y. Tserkovnyak, G.S.D. Beach, E.E. Fullerton, C. Leighton, A.H. MacDonald, D.C. Ralph, D.A. Arena, H.A. Dürr, P. Fischer, J. Grollier, J.P. Heremans, T. Jungwirth, A.V. Kimel, B. Koopmans, I.N. Krivorotov, S.J. May, A.K. Petford-Long, J.M. Rondinelli, N. Samarth, I.K. Schuller, A.N. Slavin, M.D. Stiles, O. Tchernyshyov, A. Thiaville, B.L. Zink. Rev. Mod. Phys. **89**, *2*, 025006 (2017).
[4] R. Khymyn, I. Lisenkov, V. Tiberkevich, B.A. Ivanov, A. Slavin. Sci. Rep. **7**, 43705 (2017).
[5] O.R. Sulymenko, O.V. Prokopenko, V.S. Tiberkevich, A.N. Slavin, B.A. Ivanov, R.S. Khymyn. Phys. Rev. Appl. **8**, *6*, 064007 (2017).
[6] E.A. Karashtin. Pis'ma v ZhETF **112**, *2*, 121 (2020). (in Russian).
[7] A.M. Kadigrobov, Z. Ivanov, T. Claeson, R.I. Shekhter, M. Jonson. Europhys. Lett. **67**, *6*, 948 (2004).
[8] Yu.V. Gulyaev, P.E. Zilberman, A.I. Panas, S.G. Chigarev, E.M. Epstein. Radiotekhnika i elektronika, **5**, 715 (2010). (in Russian)
[9] A.M. Kadigrobov, R.I. Shekhter, M. Jonson. Low Temp. Phys. **38**, *12*, 1133 (2012).
[10] Yu.V. Gulyaev, P.E. Zilberman, E.M. Epstein, R.J. Elliott. Radiotekhnika i elektronika, **48**, *9*, 1030 (2003). (in Russian)
[11] Yu.V. Gulyaev, P.E. Zilberman, A.I. Krikunov, A.I. Panas, E.M. Epstein. Pis'ma v ZhETF **85**, *3*, 192 (2007). (in Russian).
[12] Yu.V. Gulyaev, P.E. Zilberman, S.G. Chigarev, E.M. Epstein. Radiotekhnika i elektronika, **55**, 1211 (2010). (in Russian)
[13] A.M. Kadigrobov, R.I. Shekhter, S.I. Kulinich, M. Jonson, O.P. Balkashin, V.V. Fisun, Yu.G. Naidyuk, I.K. Yanson, S. Andersson, V. Korenivski. New J. Phys. **13**, *2*, 023007 (2011).
[14] Yu.V. Gulyaev, P.E. Zilberman, G.M. Mikhailov, S.G. Chigarev. Pisma v ZhETF **98**, *11*, 837 (2013). (in Russian).
[15] V. Korenivski, A. Iovan, A. Kadigrobov, R.I. Shekhter. Europhys. Lett. **104**, 27011 (2013).
[16] E.A. Vilkov, G.M. Mikhailov, S.A. Nikitov, A.R. Safin, M.V. Logunov, V.N. Korenivskii, S.G. Chigarev, L.A. Fomin. FTT **61**, *6*, 1021 (2019). (in Russian).
[17] E.A. Vilkov, S.G. Chigarev, I.V. Malikov, L.A. Fomin. FTT **63**, *9*, 1193 (2021). (in Russian).
[18] I.A. Dzyaloshinsky. J. Phys. Chem. Solids **4**, 241 (1958).
[19] T. Moriya. Phys.Rev. **120**, *1*, 91 (1960).
[20] Yu.V. Gulyaev, P.E. Zilberman, A.I. Panas, E.M. Epstein, S.G. Chigarev. Tverdotel'nyi istochnik elektromagnitnogo izlucheniya. Patent RF № 2464683. Byull. No. 29, 20.10.2012. (in Russian).
[21] A.I. Panas, S.G. Chigarev, E.A. Vilkov, O.A. Byshevky-Konopko, D.L. Zagorsky, I.M. Doludenko. Izv. RAN. Ser. fiz. **86**, *7*, 1013 (2022). (in Russian).
[22] S.G. Chigarev, L.A. Fomin, D.P. Rai, E.A. Vilkov, O.A. Byshevsky-Konopko, D.L. Zagorsky, I.M. Doludenko, A.I. Panas. SPIN **13**, *1*, 2350010 (2023).

Translated by E.Ilyinskaya